

were able to satisfactorily fit the CIV emission profile at all epochs by varying only two parameters, namely the intensity of the two broad Gaussian components. We found it reasonable to try a similar model in the case of NGC 4151. In this case, the widths of the two resolved components are $\sigma = 7$ and 15 \AA respectively. With this model, we have a good fit for all epochs. Indeed the fit included an unresolved Gaussian component in absorption for which we were able to get the depth at each epoch. We have plotted the depth of the absorption component versus the strength of the underlying component; these two quantities are more or less proportional, but with a rather large scatter; we obtained a much better correlation when plotting the depth of the absorption line versus the total intensity of the emission (continuum plus the two broad emission components) at the wavelength of the absorption line (Fig. 6). The CIV equivalent width is found to be constant and equal to 7.5 \AA .

It has been claimed (12) that the equivalent width of NV λ 1240 strongly correlates with the continuum flux at 2500 \AA . However, this line appears on the blue wing of the NV emission line and on the red wing of the very strong Ly α emission line. Therefore, the measurement of its strength strongly depends on the modelling of the Ly α emission and we have found it impossible to get measurements with a useful accuracy. Therefore we are not able to confirm the result quoted above and we strongly suspect it.

All the available data are compatible with the following conclusions.

- All observed absorption lines in the UV spectrum of NGC 4151 are produced in one or several (as suggested by the splitting of the He I λ 3889 absorption line into three components, Anderson 1974); with the probable exception of OI λ 1302 which may be mainly of galactic origin;
- these clouds have a high density ($N_e > 10^{8.5} \text{ cm}^{-3}$) as shown by the presence of several absorption lines from metastable levels (C III, Si III, He I);
- the continuum source is double with one constant component and one variable;

- the absorbing clouds cover the variable continuum source and the broad emission line region;
- taking into account the fact that the non-variable continuum source is not covered by the absorbing cloud, the equivalent width of all the absorption lines is constant.

Acknowledgements

It is a pleasure to thank W. Huchtmeier and O. Richter for obtaining the 21 cm spectrum in the direction of NGC 4151. We are grateful to E. Zuiderwijk for putting at our disposal his line-fitting computer programme.

References

1. Seyfert, C.K. 1943, *Astrophysical Journal* **97**, 28.
2. Anderson, K.S. 1974, *Astrophysical Journal* **189**, 195.
3. Boggess, A. et al. 1978, *Nature* **275**, 372.
4. Penston, M.V. et al. 1981, *Monthly Notices of the Royal Astronomical Society* **196**, 857.
5. Bromage, G.E. et al. 1982, ESA SP-176, p. 533.
6. Ulrich, M.H. et al. 1984, *Monthly Notices of the Royal Astronomical Society* **206**, 221.
7. Penston, M.V., Clavel, J., Sniijders, M.A.J., Boksenberg, A., and Fosbury, R.A.E. 1979, *Monthly Notices of the Royal Astronomical Society* **189**, 45P.
8. Barr, P., White, N.E., Sandford, P.W., and Ives, J.C. 1977, *Monthly Notices of the Royal Astronomical Society*, **181**, 43P.
9. Holt, S. S., et al. 1980, *Astrophysical Journal* **241**, L 13.
10. Schreier, E.J., Gorenstein, P., and Feigelson, E.D. 1982, *Astrophysical Journal* **261**, 42.
11. Johnston, K.J., Elvis, M., Kjer, D., and Shen, B.S.P. 1982, *Astrophysical Journal* **262**, 61.
12. Bromage, G.E. et al. 1984, preprint.
13. Anderson, K.S., and Kraft, R.P. 1969, *Astrophysical Journal* **158**, 859.
14. Boksenberg, A., and Penston, M.V. 1976, *Monthly Notices of the Royal Astronomical Society* **177**, 127P.
15. Ulrich, M.H. et al. 1980, *Monthly Notices of the Royal Astronomical Society* **192**, 561.

The Nature of Subdwarf B Stars

U. Heber and K. Hunger, *Institut für Theoretische Physik und Sternwarte der Christian-Albrechts-Universität, Kiel*

Introduction

Subdwarf B stars from the blue end of the horizontal branch. They occur both in the field and in globular clusters. A large fraction of the field sdB's (as well as sdO stars) has been found accidentally, during a search for faint blue objects (quasars) at high galactic latitudes, whereas the cluster sdB's are the result of a systematic search. The total number of subdwarf B stars presently known is estimated to roughly 70. It is anticipated that the true number is much larger.

Subdwarf B stars have colours and hence temperatures which are typical for B stars, but which, in some cases, even reach up to 40,000 K and beyond. The latter are more precisely defined as sdOB stars. At the temperatures in question, the neutral helium line λ 4471 should be prominent in the spectrum of subdwarf B stars. However, in most sdB's this line is barely seen at moderate resolution, or even absent (Fig. 1). The main features are the strong and Stark broadened Balmer absorption lines, besides which hardly any other line can be traced. Most sdOB stars (e.g. Feige 110, Fig. 1) show He II,

λ 4686 \AA , but the weakness of helium lines distinguishes subdwarf B and OB stars from the hot subdwarf O stars (Fig. 1). The latter are known to be helium rich (Hunger and Kudritzki, 1981). Do we then have to conclude that subdwarf B (and OB) stars are deficient in helium—a conclusion that obviously would be in conflict with the idea of horizontal branch stars as being evolved stars? Or is the definition of subdwarf B stars as horizontal branch stars to be questioned? For the discussion of the evolutionary status, a necessary prerequisite is the precise knowledge of the fundamental stellar (atmospheric) parameters like effective temperature, gravity and hydrogen-to-helium content.

Spectral Analysis

Spectral analysis yields the wanted parameters. The best way to determine the effective temperature of a given star is by studying profiles and equivalent widths of an element that is observed in 2 stages of ionization. Only if one has the properly chosen model atmosphere which is defined by T_{eff} , besides g

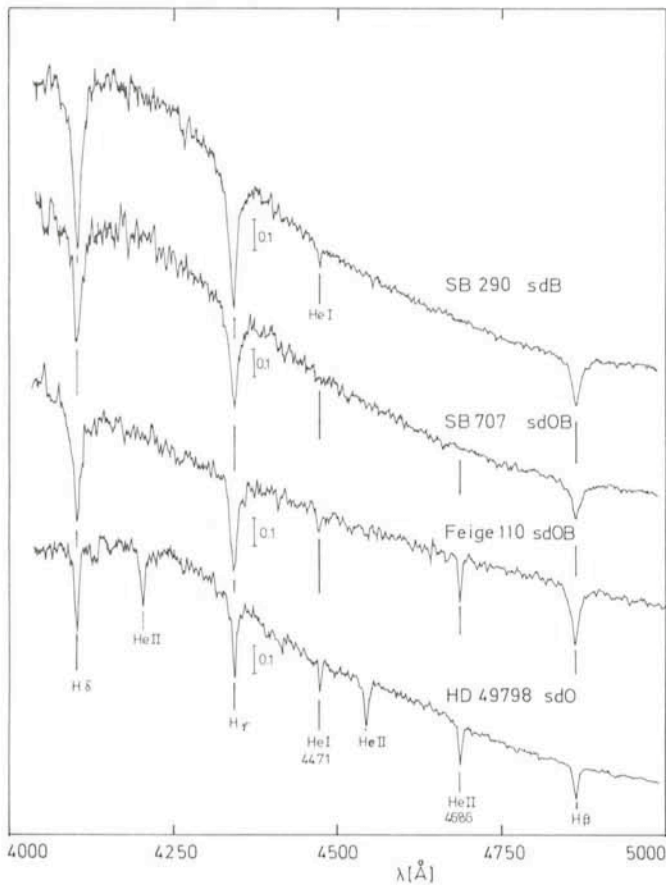


Fig. 1: Medium resolution IDS spectrograms (58 \AA/mm) of the sdB star SB 290, the sdOB SB 707 and Feige 110, and the sdO HD 49798. 10 % intensity at H_γ is indicated by a vertical bar. (The spectra are flat field corrected, but not calibrated to absolute fluxes.)

and H/He ratio, one is able to reproduce the observed equivalent widths of both stages of ionization with one single abundance of the element considered. In essence, this method is equivalent to the temperature determination from spectral type. The other method makes use of colours. As we have just seen that subdwarf B stars show hardly any metal lines and none in two stages of ionization, one is left with these "colour temperatures". The well-known study of a large sample of subdwarf B stars by Newell (1973) is based on intermediate band colour indices, and in the comprehensive analysis by Greenstein and Sargent (1974), use is made of broadband colours. Similarly, in the early analysis of the two brightest subdwarf B stars spectral scans were compared (see Baschek, 1975).

"Colour temperatures" are reliable whenever the colours are sampled at wavelengths which contribute significantly to the radiated energy. When the temperatures exceed 20,000 K, colours taken in the optical yield decreasingly less reliable temperatures as the bulk of radiation shifts towards the UV. Here is where UV colours become a necessity.

The Importance of IUE

As for B stars, the main flux is carried in the IUE band; IUE is the ideal instrument for the determination of effective temperatures. Fig. 2 shows the observed spectra of 3 subdwarf B stars: SB 459 (top), LB 1559 (middle) and SB 290 (bottom). They cover the broad wavelength range from 1200 Å to 5500 Å. The IUE spectra are at low resolution, and for SB 459 and LB 1559 in both wavelength ranges. For SB 290, fluxes measured

with the satellite TD 1 (marked by error bars) have been added. At the long wavelengths, Johnson and Strömgren colours are shown. The way the IUE spectra are corrected for interstellar reddening and how, simultaneously, the angular diameter θ and the effective temperature T_{eff} is determined, is described in detail in the paper by Heber et al. (1984). The principle, however, can be understood from Fig. 2: For SB 459, three theoretical fluxes are reproduced: for $T_{\text{eff}} = 22,500 \text{ K}$, $25,000 \text{ K}$, and $27,500 \text{ K}$, respectively. The fluxes are from fully line blanketed LTE models (Kurucz, 1979). Even taking into account the internal error of the IUE calibration (which is shown as vertical bar at the left end of Fig. 2), it is clear that the two temperature extremes can be ruled out, and that $25,000 \text{ K} \pm 1,200 \text{ K}$ can be adopted with confidence.

The IDS Spectrograms

After having determined T_{eff} rather unambiguously (the procedure is largely independent of gravity and He/H ratio) the gravities can be determined straightforwardly from the profiles of H_γ and H_β . In Fig. 3, our three examples, SB 459 (top), LB 1559 (middle) and SB 290 (bottom), are shown for comparison between theory (dashed) and observation (full drawn). The best fits have been obtained for $\log g = 5.3$ (SB 459), 5.2 (LB 1559) and 5.5 (SB 290), the error estimate being ± 0.2 .

In the same manner, the helium content can be obtained from $\lambda 4471$, if present. Otherwise upper limits are inferred. As it turns out, all the 19 programme stars are deficient in helium by factors varying from 25 to 100. Before we discuss this remarkable abundance anomaly, let us first turn to the (g , T_{eff}) diagram.

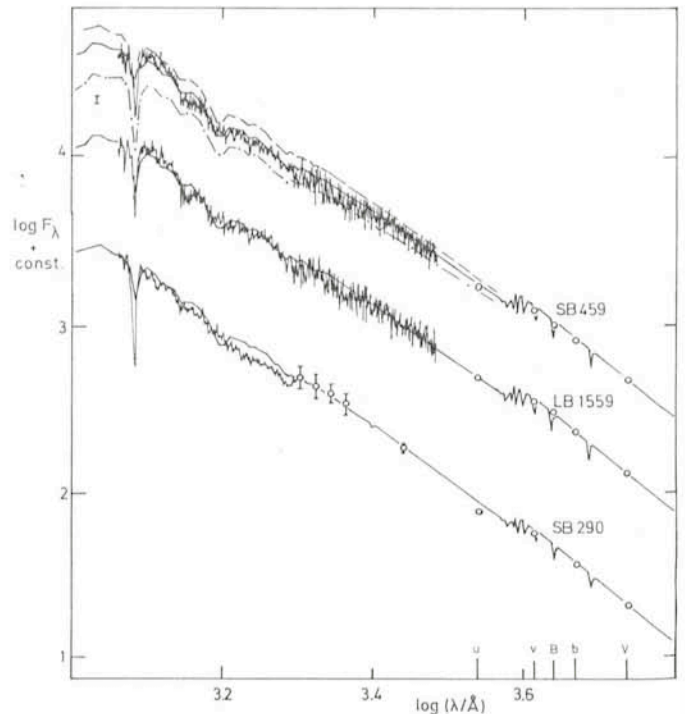


Fig. 2: Comparison of the observed UV spectra with the finally adopted models for SB 459 ($T_{\text{eff}} = 25,000 \text{ K}$), LB 1559 ($T_{\text{eff}} = 25,200 \text{ K}$) and SB 290 ($T_{\text{eff}} = 28,200 \text{ K}$). For SB 459 additional model fluxes with $T_{\text{eff}} = 27,500 \text{ K}$ (dashed), and $22,500$ (dashed dotted) are shown. The small error bar indicates the intrinsic accuracy of the IUE calibration (10%). Open circles: Johnson and Strömgren colours. TD1-fluxes are shown with error bar.

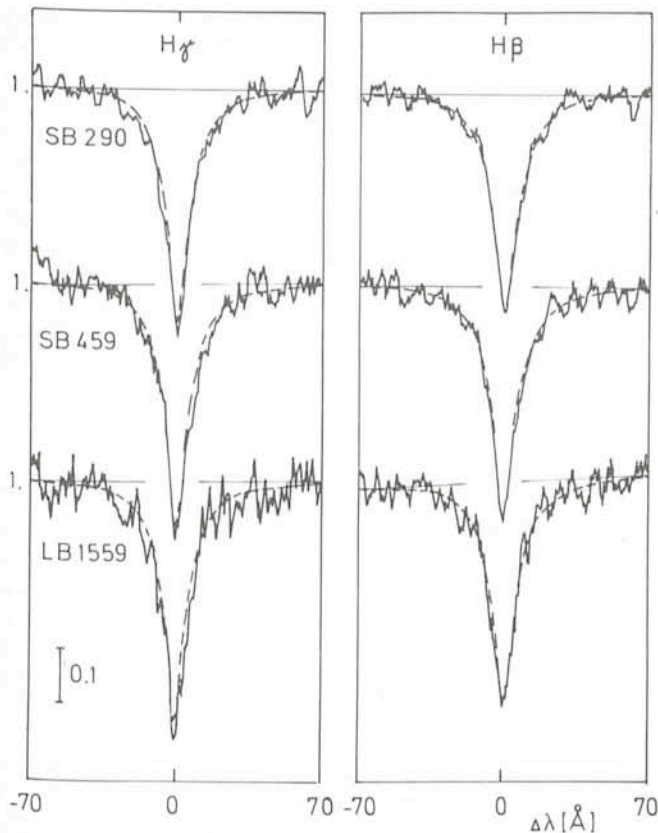


Fig. 3: Comparison of observed profiles of H_γ and H_β with theory for SB 290, SB 459 and LB 1559. The dispersion is 58 \AA/mm . 10% intensity is indicated by a vertical bar.

(g , T_{eff}) Diagram

The (g , T_{eff}) diagram, the morphological equivalent to the H. R. diagram, allows the direct comparison between the observations and the results of stellar interior calculations. In Fig. 4, the presently analysed subdwarf B stars (triangles) and their hot counterparts, the subdwarf OB stars (circles) are shown. The accuracy of the observed temperatures and gravities is characterized by crossed error bars (top). The zero-age helium main sequence (He-m.s.) runs at the bottom, while the zero-age horizontal branch (H.B.) extends downwards from the upper right corner. For clarity, the latter is reproduced only for one mass fraction of helium, $Y = 0.25$. The H. B. stars are assumed to have core masses of $M_c = 0.475 M_\odot$. The envelope masses M_e are very small, comprising only $0.06 M_\odot$ at the cool end to $0.005 M_\odot$ at the hot end. True H. B. stars exist only down to $M_e = 0.02 M_\odot$ (Gross, 1973), because below this mass, the hydrogen shell burning becomes negligible. The sequence from $M_e = 0.005 M_\odot$ to $M_e = 0 M_\odot$ is interpolated (dashed curve). Stars with $M_e < 0.02 M_\odot$ may be termed generalized helium main-sequence stars in the sense that they have only one single central source of energy left, as the true helium m.s. stars.

The evolution of a helium m.s. star proceeds at a drastically different path than that of an H. B. star. While the former moves horizontally towards hotter temperatures, the latter moves vertically towards lower gravities: the corresponding arrows correspond to an evolutionary time of $1.4 \cdot 10^8$ years, for both evolutions.

The (g , T_{eff}) diagram allows an immediate conclusion as to the evolution of our sample of subdwarf B stars: they have reached their present location along a horizontal vector from the (zero age) extended horizontal branch with $M_e < 0.02 M_\odot$,

i. e. from the generalized helium main sequence. The time that elapsed after they left the sequence until helium core exhaustion is of the order of 10^8 years.

Even more dramatically appears the conclusion one has to draw with regard to the subdwarf OB stars: a major fraction—and these are the stars with gravities of the order of 10^{+6} —are true helium main-sequence stars, with $M_e < 10^{-3} M_\odot$ (e.g. SB 707). These are up to now the only bona fide helium main-sequence stars that are known. However, there is one dilemma: we have seen above that these stars are helium depleted rather than helium rich. The sdOB SB 707 even does not show any helium lines in the visual (see Fig. 1), but, nevertheless, is regarded as a helium main-sequence star. (Those sdOB's with smaller gravities, e.g. Feige 110, have evolved from the generalized helium main sequence [see below]).

The Helium Main-Sequence Stars (sdOB's) and Their Photospheric Helium Content

It is known that the envelopes of white dwarfs are composed of almost pure helium, even those of the apparently hydrogen-rich white dwarfs of type DA (Dziembowski and Koester, 1981). The very small amount of hydrogen left to these stars floats atop the helium layer due to the enormous gravity present and thus becomes the dominant spectral feature. A similar situation holds for the subdwarf OB stars (Hunger and Kudritzki, 1981). Diffusion in the presence of strong gravity forces the available hydrogen to the surface and hence mimics a hydrogen star, even in those cases where the outer layers are mainly composed of helium. Clearly the same action of diffusion is seen in our subdwarf B stars.

Metal Abundances

Diffusion not only affects helium, but also the metals. Hence conclusions with regard to evolution (e.g. N enrichment

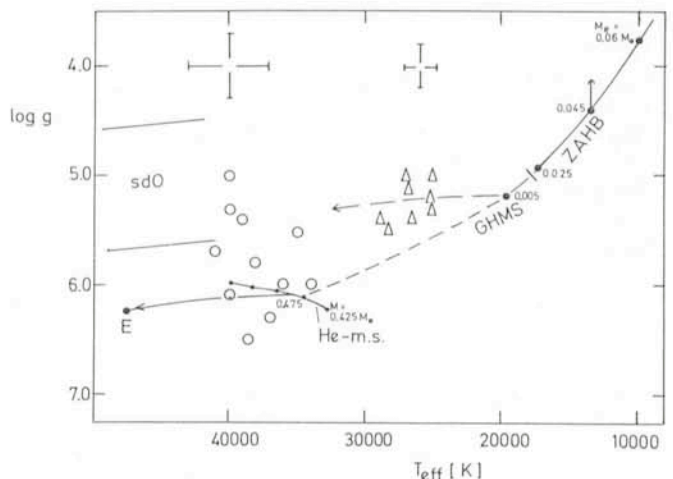


Fig. 4: Position of sdB (Δ) and sdOB stars (O) in the ($\log g$, T_{eff}) plane (typical errors are indicated by crossed bars). Also shown are the helium main sequence plus the evolutionary path of a $0.5 M_\odot$ pure helium star up to core helium exhaustion (point E), and ZAHB models for $Y = 0.25$ from Gross (1973). The models are labelled with their envelope mass M_e . The dashed line is an interpolation for very low envelope masses ($M_e \leq 0.005 M_\odot$). The borderline (at $M_e = 0.02 M_\odot$) between canonical ZAHB stars and generalized helium main-sequence stars (GHMS) is indicated by a tick mark. The evolution of (zero age) GHMS stars up to helium core exhaustion proceeds along the (horizontal) dashed vector while the evolution of a canonical ZAHB star proceeds along the vertical vector.

through the CNO cycle, stellar population) cannot simply be drawn from metal abundances.

The optical spectra hardly contain metal lines, whereas in the UV a large number of lines is present. High resolution IUE spectrograms of 3 sdOB stars (HD 149382, Feige 66 and Feige 110) have been analysed with the result that silicon is deficient in all 3 stars, by as much as a factor 40,000 (!) in HD 149382. Carbon likewise is deficient in Feige 110, by a factor 300,000 (!), but only moderately deficient (factor of ~ 100) in the 2 other stars, whereas nitrogen appears to be (nearly) solar in all 3 stars. In contrast to the sdOB's, silicon appears (almost) solar in the subdwarf B stars.

Some of these strange abundance anomalies can be understood, for instance the deficiency of silicon: at temperatures occurring near the bottom of the photospheres in subdwarf OB stars, silicon is ionized to Si^{4+} . This ion has a noble gas electron configuration with small absorption cross sections. Radiation that otherwise would force the ion upwards can no longer balance gravitation. As a consequence, the ion sinks below the photosphere (Baschek et al., 1982). A complete and quantitative theory, however, is lacking, and one is presently left with a more or less confusing picture of strange abundance patterns. All the information hidden there and being of great potential use in defining the momentary and past state of the photospheres in those subdwarfs, cannot be exploited at present.

Evolution

From the (g, T_{eff}) diagram (see above) it was concluded that subdwarf B and OB stars form the blue extension of the horizontal branch towards higher temperatures. After helium core exhaustion they evolve at constant gravity and eventually reach the domain of subdwarf O stars. This means that the (g, T_{eff}) domain, which is occupied by subdwarf O stars, is also shared by evolved subdwarf B stars. How can these two classes be separated?

It is known that subdwarf O stars are helium rich. They have

temperatures above 40,000 K (Hunger and Kudritzki, 1981). At these temperatures, the He II convection zone extends up to the photosphere and thus inhibits diffusion which would dilute helium. But once helium is depleted as in our sdB sample, He II convection cannot work and hence a subdwarf B star, when crossing the 40,000 K boundary, stays helium poor (Groth and Kudritzki, 1983). For subdwarf O stars, the situation is different: they start from the (canonical) horizontal branch, i.e. with masses between 0.5 and 0.6 M_{\odot} , and hydrogen-rich shell masses in excess of 0.02 M_{\odot} . They move upwards in the (g, T_{eff}) plane along a "Sweigart" track, attaining gravities which are too small for diffusion, and eventually experience shell flashes. When they reach the sdO domain, they have already mixed helium to the surface and thus convection becomes possible. This means true subdwarf O stars can be distinguished from evolved sdB (and sdOB) stars by their helium content. So far, 3 objects are known whose effective temperatures are in excess of 40,000 K and whose helium contents are subsolar (Heber and Hunger, in preparation). Those are, according to the above described picture, old evolved subdwarf B stars.

References

- Baschek, B.: 1975, in *Problems in Stellar Atmospheres and Envelopes*, eds. Baschek, B., Kegel, W. H., Traving, G., Springer, Berlin, Heidelberg, New York, p. 101.
- Baschek, B., Kudritzki, R. P., Scholz, M., Simon, K. P.: 1982, *Astronomy and Astrophysics* **108**, 387.
- Dziembowski, W., Koester, D.: 1981, *Astronomy and Astrophysics* **97**, 16.
- Greenstein, J. L., Sargent, A. I.: 1974, *Astrophysical Journal, Suppl.* **28**, 157.
- Gross, P. G.: 1973, *Monthly Notices Roy. Astron. Soc.* **164**, 65.
- Groth, H. G., Kudritzki, R. P.: 1983, *Mitt. d. Astron. Ges.* **60**, 308.
- Heber, U., Hunger, K., Jonas, G., Kudritzki, R. P.: 1984, *Astronomy and Astrophysics* **130**, 119.
- Hunger, K., Kudritzki, R. P.: 1981, *The Messenger* **24**, 7.
- Newell, E. B.: 1973, *Astrophysical Journal, Suppl.* **26**, 37.

Stellar Metallicity Gradient in the Direction of the South Galactic Pole Determined from Walraven Photometry

Ch. F. Trefzger, *Astronomisches Institut der Universität Basel, Switzerland*

J. W. Pel and A. Blaauw, *Kapteyn Astronomical Institute, Groningen, the Netherlands*

Introduction

It has been known for a while that the stellar population in our Galaxy changes drastically as a function of distance from the galactic plane—the disk is composed mostly of relatively young stars with solar metal abundances and small velocity dispersions whereas the average metallicity drops and the age increases as we look at stars deeper in the halo. These findings were interpreted by Eggen et al. (1962, *Astrophysical Journal* **136**, 748) in terms of their rapid collapse model of the protogalaxy and the subsequent formation of the disk. However, for a detailed model of the evolution of the Galaxy we need a much broader observational basis, viz. knowledge of the parameters stellar density, metallicity, age and velocity dispersion as a function of distance from the galactic plane. Several attempts have been made to reach this goal.

The Basel halo programme has been described and initiated by Becker (1965, *Zeitschr. f. Astrophys.* **62**, 54). The aim was to study the stellar density function in different halo directions (mostly Selected Areas) in a meridional plane perpendicular to the disk containing the galactic centre and the sun. The programme is based on deep Palomar Schmidt plates taken with the three filters of the RGU system. It is well known that metal-poor stars show UV excesses relative to stars with solar abundances. In the RGU system, this effect is even more pronounced than in the UVV system, and it can be used to separate the metal-poor halo stars from the solar abundance disk stars statistically. The metallicities of the halo stars in the Basel Survey have been estimated on the basis of their colours by Trefzger (1981, *Astronomy and Astrophysics* **95**, 184).

The nearby field star population at the galactic poles has been investigated by Blaauw and Garmany (1975, in Proceed-